

STUDY ON AIR-SEA HEAT EXCHANGE MECHANISM IN EL NINO AND LA NINA EVENTS

Ma Kaiyu (马开玉),

Department of Atmospheric Sciences, Nanjing University, Nanjing 210008

Yao Huadong (姚华栋) and Jiang Dayong (姜达雍)

Chinese Academy of Meteorological Sciences, Beijing 100081

Received January 24, 1992; revised September 30, 1992

ABSTRACT

$2^{\circ} \times 2^{\circ}$ mean monthly COADS grid data in 1974 and 1987 of El Nino and La Nina years are used to compute the sensible and latent heat fluxes, the net longwave radiation, the incident solar radiation and heat budget on the tropical Pacific surface (30°S — 30°N). The difference of the heat budget between El Nino and La Nina mainly occurred on the equatorial ocean surface, especially the water area west of Ecuador and Peru. During El Nino, the sensible and latent heat exchange increased, the net longwave radiation and incident solar radiation decreased and the net gain(loss) of heat reduced(increased) on the ocean surface. During La Nina, the circumstances were opposite. Finally an ideal model of air-sea heat exchange mechanism for the El Nino-La Nina cycle is summarized.

Key words: El Nino, La Nina, air-sea heat exchange, COADS grid data

I. INTRODUCTION

In the climate system, ocean and atmosphere are coupled each other through thermal, dynamical and hydrological processes. El Nino and La Nina which occur in the eastern equatorial Pacific are the most significant events of ocean-atmosphere coupling. Numerous studies have suggested that El Nino has enormous influence on the atmospheric circulation, especially on the western subtropical Pacific high, the thermal fields in the southern and eastern Asia and climatic anomalies in many regions. Therefore it is not surprising that meteorologists and oceanographers in the world focus their attention on the studies of the regularity and physical mechanism of El Nino in an attempt to provide reliable information and physical evidence for the predictions of El Nino occurrence and climate disasters in the future.

There are numerous fruits on the dynamical researches of El Nino and La Nina events. Research by Bjerknes(1966) has suggested that the weakening and temporary elimination of equatorial easterlies over the eastern and central Pacific bring about a cessation of equatorial upwelling which in turn causes the occurrence of above-normal surface water temperature in the tropical Pacific from the American coast westward to the international date line. Modeling studies by McCreary et al.(1983; 1984) have indicated that El Nino event is the result of warm equatorial Kelvin wave propagating eastward and warm Rossby wave being reflected from east boundary. Schopf and Suarez(1988) suggested an El Nino-La Nina cycle mechanism which includes unstable ocean-atmosphere coupling with Kelvin and Rossby waves propagating. Fig.1 shows the scheme of the cycle mechanism. Data analysis and numerical modeling have found

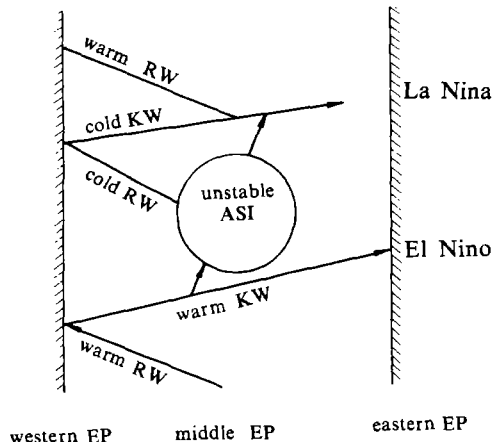


Fig.1. Scheme of unstable ocean-atmosphere interaction mechanism in El Niño-La Niña cycle. Here RW: Rossby wave; KW: Kelvin wave; EP: equatorial Pacific; ASI: air-sea interaction.

that the drought belt weakened and shrunken and precipitation increased in the eastern Pacific when sea water temperature rose in the cold water region(Rowntree, 1972; Wang et al., 1986).

In the research of air-sea heat exchange, Ramage and Hori(1981) computed the average heat budgets during El Niño and La Niña in the 15°S — 15°N of the eastern Pacific to the date line. They found that the maximum difference in heat budget between El Niño and La Niña appeared in the south of equatorial ocean. Zhu and Yang(1990) have analysed the sensible and latent heat fluxes in the Indian and Pacific Oceans during the developing and ending months of the El Niño event in 1983. They found that the distributions of sensible and latent heat fluxes in the Indian Ocean were similar to those in normal years. These researches have provided useful references for understanding the influence of sea temperature anomaly on the atmosphere. But further study is needed because only fewer items of heat exchanges were computed or limited region was covered in their work.

In this paper, the years of 1987 in El Niño and 1974 in La Niña have been selected to compute the incident solar radiation, net longwave radiation, sensible and latent heat fluxes and heat budget on the tropical Pacific surface (30°S — 30°N). It is expected that this study could be helpful for understanding the mechanism of air-sea heat exchange in the El Niño-La Niña cycle and improving the related climate modeling.

II. DATA AND COMPUTATIONAL METHOD

1. Data

From Monitoring Group of ENSO(1989), in recent years the El Niño occurring during Oct. 1986—March 1988 was a significant oceanic event which continued 18 months with the maximum average monthly above-normal surface water temperature by 1.5°C in the eastern equatorial Pacific (0° — 10°S , 180° — 90°W) and the La Niña during Sept. 1973—Jan. 1975 was a stronger La Niña event which continued 17 months with the maximum average monthly below-normal surface temperature by -1.5°C . In this paper we select them to compute the heat exchange and budget on the tropical Pacific surface (30°S — 30°N) by using $2^{\circ} \times 2^{\circ}$ grid COADS

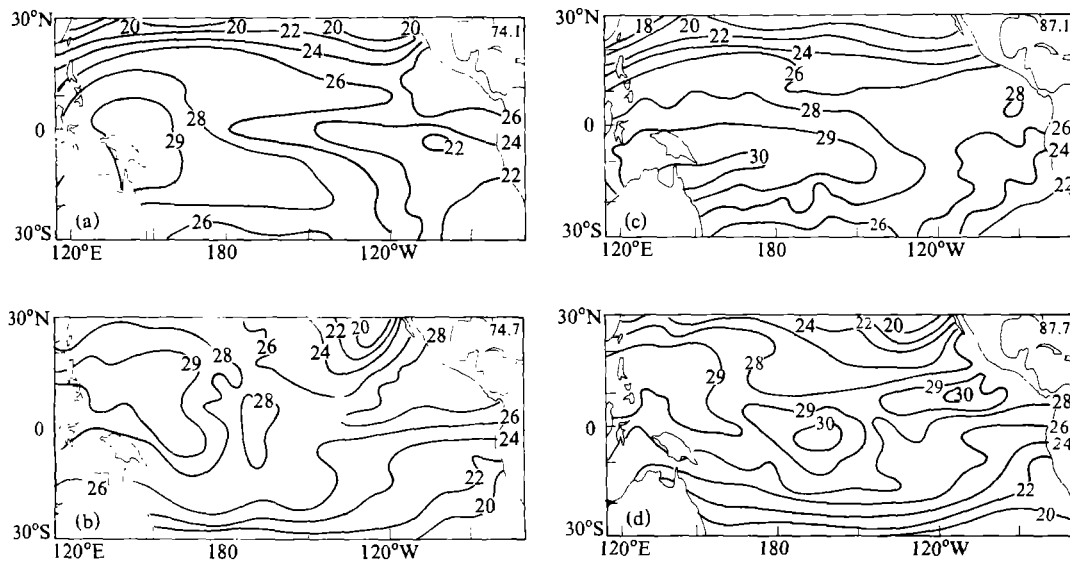


Fig.2. Distributions of sea surface temperature($^{\circ}\text{C}$) on the tropical Pacific for January and July of 1974(a, b) and 1987(c, d).

data in 1974 and 1987. Fig.2 shows the distributions of sea surface temperature in January and July of 1974 and 1987.

2. Computational Method

Sensible and latent heat fluxes are given by

$$Q_c = \rho C_d C_p (T_s - T_a) V, \quad (1)$$

$$Q_e = \rho C_d L (q_s - q_a) V, \quad (2)$$

where $\rho = 1.175 \text{ kg m}^{-3}$ is air density; $C_p = 1.0048 \text{ J g}^{-1} \text{ K}^{-1}$, the specific heat at constant pressure; $L = 2.4981 \times 10^3 \text{ J g}^{-1}$, the latent heat evaporation; T_s and T_a the sea surface temperature and air temperature; q_a and q_s the surface specific humidity and the saturation specific humidity corresponding to the sea surface temperature, V the scalar mean wind speed, C_d the exchange coefficient related to wind speed and stability (Bunker, 1976).

Net longwave radiation is computed by

$$Q_l = \varepsilon \sigma T_a^4 (0.39 - 0.056 \sqrt{q_a}) (1 - Kn^2) + 4\varepsilon\sigma T^3 (T_s - T_a), \quad (3)$$

where $\sigma^2 = 5.67 \times 10^{-8} \text{ W m}^{-2} \text{ K}^{-4}$ is Stefan-Boltzmann's constant, $\varepsilon = 1$ the emissivity, n the fraction of total cloud cover, K the parameter varying with latitude (Table 1).

Incident solar radiation flux is

$$Q_s = Q_o (1 - (a + bn)n) (1 - r), \quad (4)$$

where the values of Q_o being average monthly total solar radiation flux arrived at sea surface under clear sky, are based on Budyko (1974), $b = 0.38$, a is the parameter varying with latitude (Table 1) and r the average albedo of sea surface to solar radiation (Table 2).

Heat budget on ocean surface is given by

$$Q_b = Q_s - (Q_c + Q_e + Q_L), \quad (5)$$

where $Q_c + Q_e + Q_L$ denotes the total heat flux released to the atmosphere from oceans. It means that the ocean gains energy from outside when Q_b is positive; otherwise the ocean loses energy.

Table 1. Coefficient α and K (Based on Budyko, 1974)

Latitude	0°	5°	10°	15°	20°	25°	30°
α	0.38	0.40	0.40	0.39	0.37	0.35	0.36
K	0.50	0.52	0.55	0.57	0.59	0.61	0.63

Table 2. Albedo of Ocean Surface to Solar Radiation (Based on Budyko, 1974)

Latitude(N)	Jan.	Feb.	March	April	May	June	July	Aug.	Sep.	Oct.	Nov.	Dec.
0°	0.06	0.06	0.06	0.06	0.06	0.06	0.06	0.06	0.06	0.06	0.06	0.06
10°	0.06	0.06	0.06	0.06	0.06	0.06	0.06	0.06	0.06	0.06	0.06	0.07
20°	0.07	0.07	0.06	0.06	0.06	0.06	0.06	0.06	0.06	0.06	0.07	0.07
30°	0.09	0.08	0.06	0.06	0.06	0.06	0.06	0.06	0.06	0.07	0.08	0.09

III. RESULTS

El Nino and La Nina are the outgrowth of large-scale air-sea coupling. Sea water temperature anomaly would influence the oceanic and atmospheric circulation system and physical processes. Therefore the incident solar radiation, net longwave radiation, sensible and latent heat fluxes and heat budgets computed on the tropical Pacific in 1974 were the results of large-scale air-sea coupling with complicated interactions.

1. Sensible Heat

From Eq.(1), sensible heat flux could be upward (positive) or downward(negative) because of its dependence on air-sea temperature difference. Fig.3 shows the distributions of sensible heat fluxes and their differences in January and July of 1974 and 1987(figures for April and October omitted). It could be seen that in the vast tropical ocean the values of sensible heat fluxes range from 0 to 20W m^{-2} except for subtropical ocean in winter hemisphere, especially over the area close to the coast of China where the flux was over 50Wm^{-2} in January. In contrast with latent heat and longwave radiation, the sensible heat flux was relatively small.

In comparison with 1987, in January 1974 the negative flux meaning the slight downward heat transfer featured the southern side of eastern equatorial ocean, in spring the negative value area shrank eastward to the coast of Ecuador, in the summer it expanded westward and in autumn the negative flux area spread widely on the south of eastern equatorial ocean. But in 1987, the negative flux area on the southern side of eastern equatorial Pacific was very small and sometimes disappeared. On its northern side the positive centers with 30 and 20Wm^{-2}

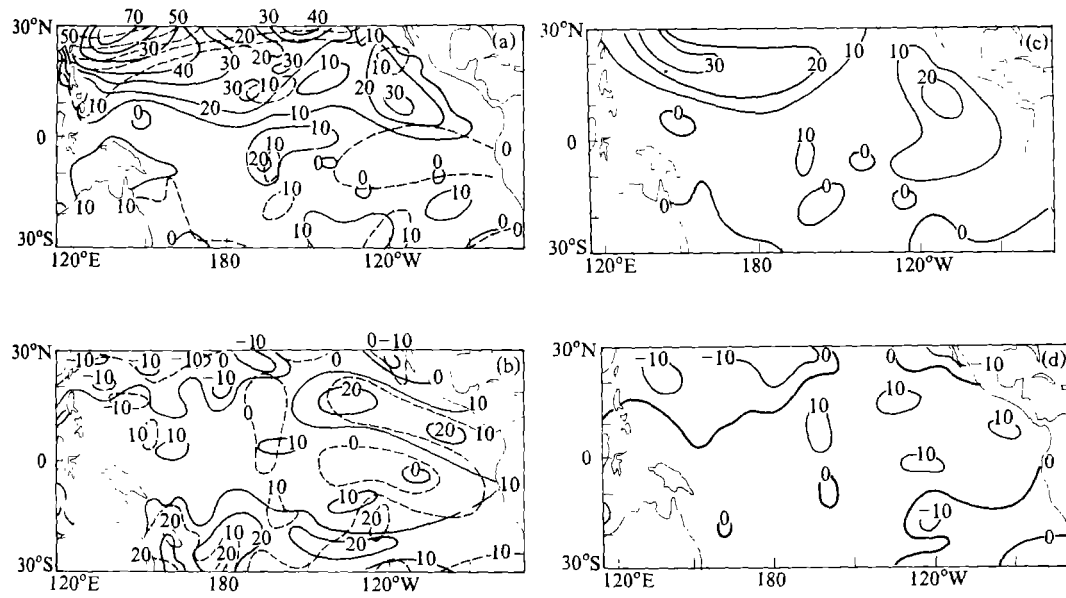


Fig. 3. Distributions of sensible heat flux (W m^{-2}) and their differences on the tropical Pacific surface for January and July of 1974 and 1987. (a) and (b) are for the heat fluxes in January and July respectively. Solid lines denote 1987 and dashed lines 1974; (c) and (d) indicate the heat flux differences between 1987 and 1974 for January and July respectively.

were found in January and July respectively. Therefore it suggests that in the eastern equatorial Pacific the response of sensible heat exchange to sea surface temperature anomaly was positive. From Figs.3c and 3d it could be seen that on the eastern equatorial Pacific $5\text{--}20 \text{ W m}^{-2}$ more(less) sensible heat was released(got) to (from) the atmosphere in 1987 as compared with that in 1974. Similar characteristics were found in the middle equatorial Pacific.

In the western equatorial Pacific sensible heat exchanges were about $5\text{--}10 \text{ W m}^{-2}$. Some scattered negative flux area could be found in January 1987 due to lower sea surface temperature there(refer to Fig.2).

In subtropical ocean, it was significant that more sensible heat was released into the atmosphere in northern subtropical Pacific in January 1987 than that in January 1974, especially near the coast of China where the maximum flux reached 110 W m^{-2} , being $10\text{--}30 \text{ W m}^{-2}$ more than that in January 1974 and near the western coast of Mexico, being $10\text{--}20 \text{ W m}^{-2}$ more sensible heat released than that in January 1974. But in these regions there gained more sensible heat and the negative values were found in the difference diagram in summer 1987. If air temperature distributions in January and July of 1974 and 1987(figures omitted) and Fig.2 are taken into account, it could be implied that the differences of sensible heat fluxes in northern subtropical Pacific are mainly determined by air temperature in wintertime and by sea surface temperature in summertime. In southern subtropical Pacific the differences of sensible heat exchanges between 1974 and 1987 were smaller than those in northern subtropical Pacific due to the influence of smaller landmass.

2. Latent Heat

As a rule the flux of latent heat is directed upward from oceans to the atmosphere and being the largest component of heat losses compared with the longwave radiation and sensible heat fluxes. From Eq.(2) it suggests that the control factors of latent heat are wind speed and vertical gradient of specific humidity on the sea surface. The gradient of specific humidity depends on air-sea temperature difference. The rising or declining of sea surface temperature would influence the air-sea temperature difference which in turn affects the vertical gradient of specific humidity.

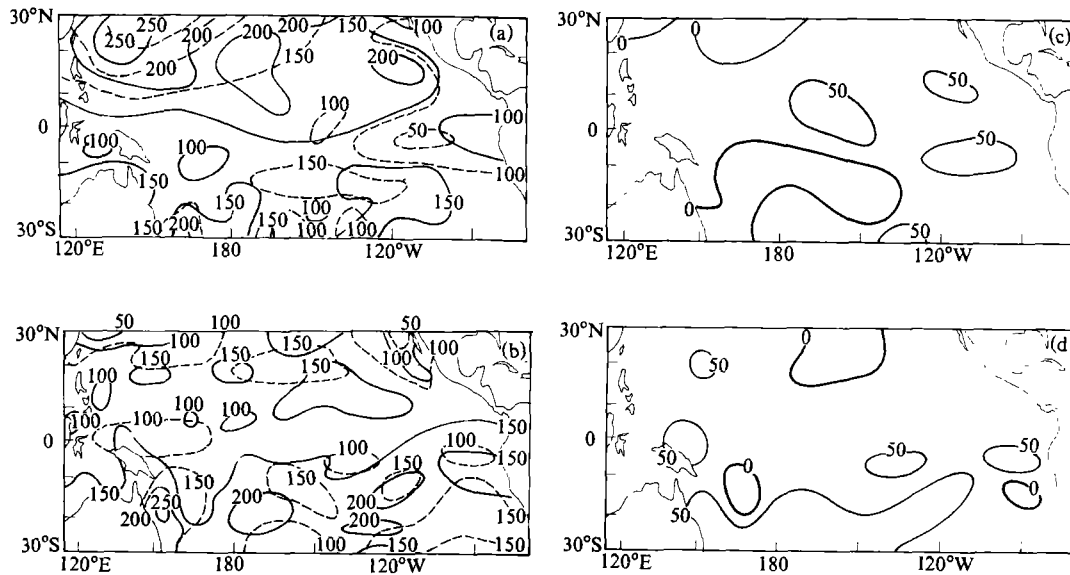


Fig. 4. As in Fig.3, except for latent heat.

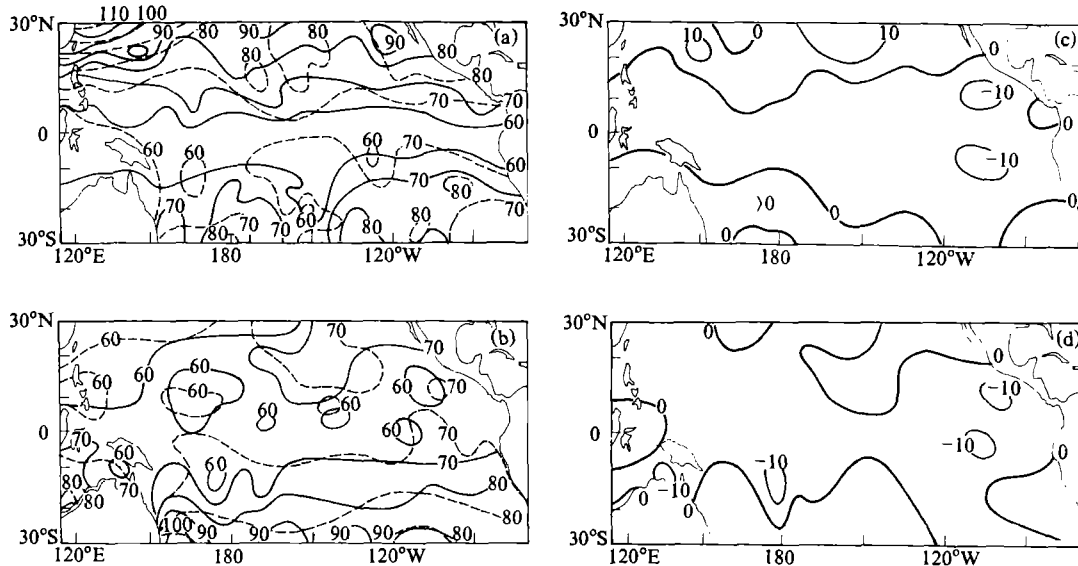


Fig. 5. As in Fig.3, except for net longwave radiation.

Fig.4 displays the latent heat fluxes and their differences in January and July of 1974 and 1987. It could be seen that more latent heat was released in January and July of 1987 on the tropical ocean surface, especially the water area west of the coast of Ecuador and Peru where the latent heat fluxes were $40\text{--}50\text{W m}^{-2}$ more than those in January and July of 1974 and as much as 4—6 times larger than the differences of sensible heat fluxes. In spring and autumn similar characteristics were found(figure omitted). In Oct. 1987, the most developed stage in the El Nino, a large latent heat flux area with over 150W m^{-2} was found close to the western coast of Ecuador where the latent heat flux was only 100W m^{-2} even below 50W m^{-2} in Oct. 1974. It could be explained that the difference between the saturation specific humidity corresponding to higher T_s and the surface specific humidity is larger when T_s is higher, even if the air-sea temperature difference is the same.

3. Net Longwave Radiation

The ocean surface continuously releases longwave radiation upward. From Eq.(3) the major factors controlling its large-scale pattern are cloud cover, specific humidity and air-sea temperature difference besides the sea surface temperature. Therefore under the air-sea coupling and interaction, the response of net longwave radiation over the ocean surface during El Nino and La Nina could be very complicated.

Fig.5 represents the net longwave radiation fluxes and their differences in January and July of 1974 and 1987. It could be seen that the low-value belts of radiation fluxes were found in the equatorial ocean and that the large amount of the radiation fluxes were released into the atmosphere from subtropical oceans in winter hemisphere. In comparing 1987 with 1974, on the equatorial ocean surface the net longwave radiation flux during El Nino was less than that during La Nina by the differences of $5\text{--}10\text{W m}^{-2}$ and there appears negative area in the difference distributions of Fig.5. In January 1974 the radiation fluxes on equatorial ocean surface ranged from 60 to 70W m^{-2} except for the ocean near Indonesia, while a low belt below 60W m^{-2} was found in January 1987. In October 1974, the ocean surface from the Date Line to the western coast of Ecuador and Peru was $70\text{--}80\text{W m}^{-2}$, but October 1987 was $60\text{--}70\text{W m}^{-2}$, some regions even below 60W m^{-2} (figure omitted).

In subtropical ocean, the characteristics of net longwave radiation differences between El Nino and La Nina were more complicated because of the influences of landmass and atmospheric circulation in the middle and high latitudes and have not been explored clearly. More data analyses and studies are needed.

4. Solar Radiation

Tropical ocean surface gains large amount of energy from the sun. From Eq.(4), the incident solar radiation on ocean surface depends on total solar radiation under clear sky Q_o , coefficient a , albedo r and cloud amount n . Owing to Q_o , a and r varying with latitude, the difference of incident solar radiation fluxes between El Nino and La Nina only depends on cloud amount n .

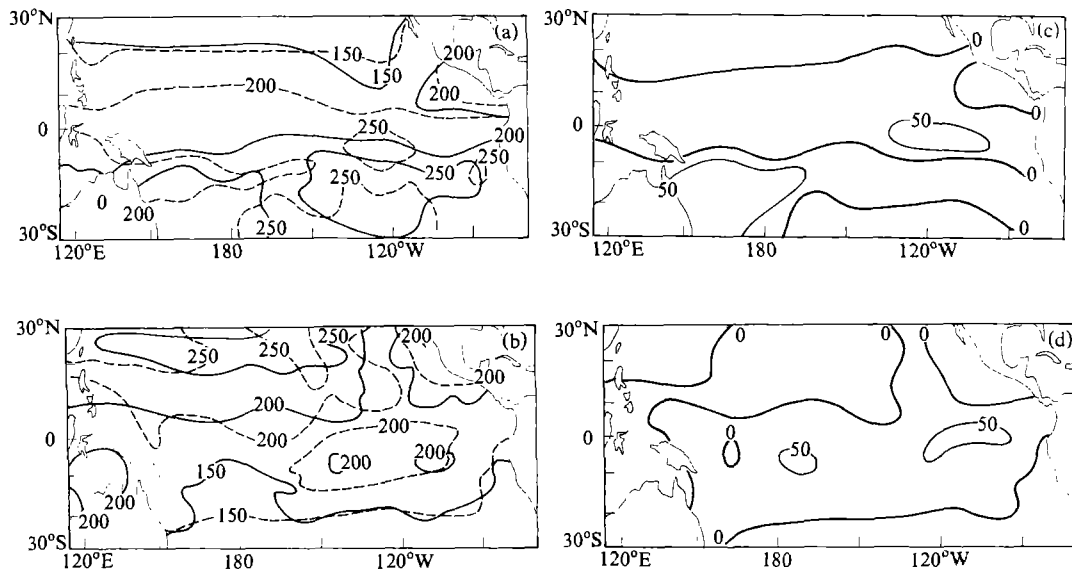


Fig. 6. As in Fig.3, except for incident solar radiation.

Fig.6 shows the distributions of solar radiation fluxes and their differences in January and July of 1974 and 1987. It reveals that in the equatorial ocean the incident solar radiation fluxes gained in January and July of 1987 were less than those in January and July of 1974 except for the ocean surface near Indonesia. In January 1974 the fluxes were $200\text{--}250\text{W m}^{-2}$ in the equatorial ocean($5^{\circ}\text{S}\text{--}5^{\circ}\text{N}$) with high value center of 250Wm^{-2} in ($110^{\circ}\text{--}140^{\circ}\text{W}$), but in January 1987 the fluxes were less than 200Wm^{-2} . In July of 1974 a wide high-flux center over 200Wm^{-2} was located in the southern side of eastern equatorial Pacific, while in July 1987 only spotted areas over 200Wm^{-2} were found. In the difference distributions (Figs.6c and 6d), the equatorial ocean surface has negative value and a negative center with -50W m^{-2} appears on the water area west of the coast of Ecuador and Peru. In transitional seasons of spring and autumn, the similar features of solar radiation flux differences between 1974 and 1987 were indicated (figure omitted). In October 1987 a low-value belt, below 200Wm^{-2} , occupied the whole equatorial ocean, but in October 1974 the fluxes over 200Wm^{-2} were spread on the vast equatorial ocean ($140^{\circ}\text{E}\text{--}90^{\circ}\text{W}$) with a high value center of 250Wm^{-2} in the area ($180^{\circ}\text{--}110^{\circ}\text{W}$). They suggest that evaporation increases, water content and convection instability in the atmosphere grow to cause increase of cloud amount and in turn result in the reduction of incident solar radiation when sea surface temperature rises abnormally.

In subtropical ocean the differences of solar radiation fluxes between El Nino and La Nina were more complicated, further study is needed.

5. Heat Budget

Heat budget on the ocean surface depends on the solar radiation absorbed and total energy released. The total energy released includes the longwave radiation, sensible and latent heat. As a result of the difference between El Nino and La Nina, in which the latent heat flux is quite

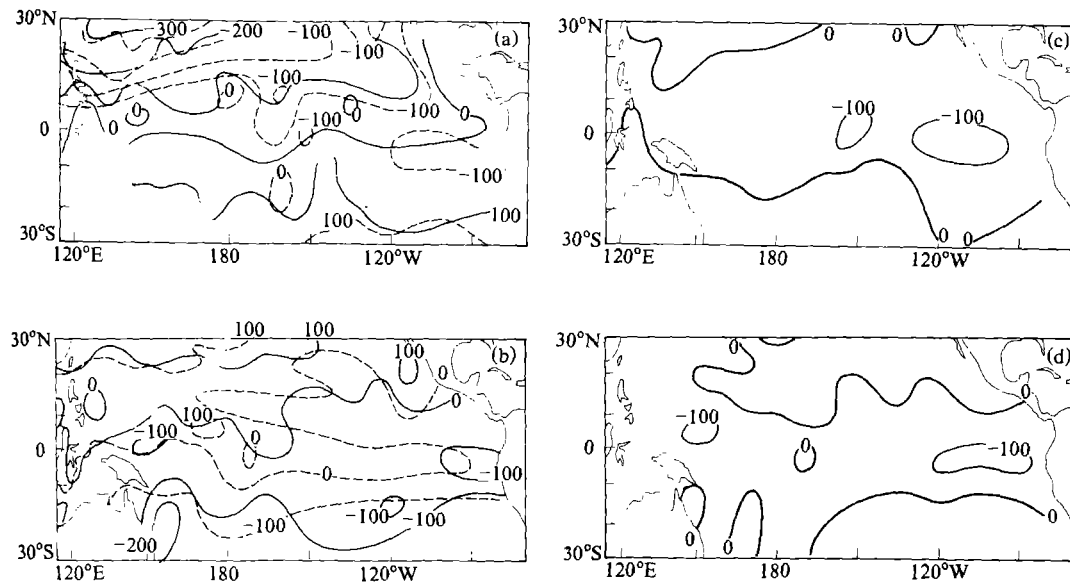


Fig. 7. As in Fig.3, except for heat budget.

different and plays an important role in heat budget, the signs of the difference of sensible heat fluxes and the difference of net longwave radiation fluxes are opposite during El Nino and La Nina, hence the difference of released total energy on ocean surface mainly reflects the difference of latent heat fluxes between El Nino and La Nina. Since the difference of sensible heat fluxes reached $10\text{--}30\text{ kW m}^{-2}$ near the coast of China, it was another factor controlling the difference of released total energy there.

Fig.7 describes the distributions of heat budget and their differences in January and July of 1974 and 1987. It could be seen that on the equatorial ocean surface the net gain (loss) of heat flux was less(more) in January and July of 1987 in comparison with that in 1974, especially the ocean surface near the coast of Ecuador and Peru where the net gain of heat flux reached over 100 W m^{-2} in January 1974 while the net loss or a little net gain of heat flux was found there in January 1987. In the difference distributions of Fig.7 there appear negative values on the equatorial ocean surface with large low-value centers of -100 W m^{-2} . Similar features of heat budget distributions were seen in transitional seasons of spring and autumn. In October 1987, the mostdeveloped stage of the El Nino, the ocean surface near the coast of Ecuador had the net loss of heat flux , but in October 1974 the vast ocean surface got a net gain of heat flux over 100 W m^{-2} .

In subtropical ocean, the characteristics of heat budget are hardly to be explored in this paper because of limited data.

IV. MECHANISM MODEL OF AIR-SEA HEAT EXCHANGE

From the analyse0s above, between El Nino and La Nina the heat budget differences were significant on the equatorial ocean surface, especially near the coasts of Ecuador and Peru

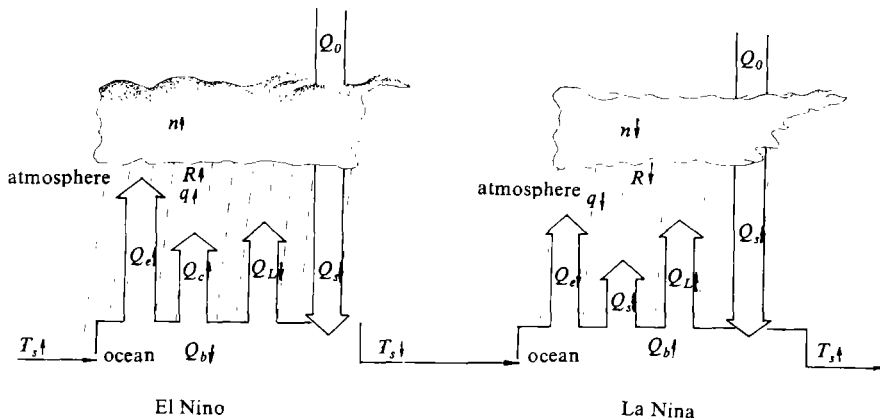


Fig. 8. Ideal model of air-sea heat exchange mechanism for El Nino-La Nina cycle.

Letter R indicates precipitation, others as in Eqs.(1)–(5).

where the differences in the net longwave radiation, the sensible and latent heat exchanges and the incident solar radiation were quite different. During El Nino the sensible and latent heat exchanges enlarged, the net longwave radiation and incident solar radiation weakened, the net gain (loss) of heat flux reduced(increased) on the equatorial ocean surface. There revealed an opposite feature in air-sea heat exchange during La Nina event. Therefore we could summarize an air-sea heat exchange mechanism of the El Nino-La Nina cycle as follows:

During El Nino, the above-normal sea surface temperature would bring about the increasing of sensible and latent heat exchanges and the rising of water vapor content and instability in the atmosphere, and in turn the growing of the cloud cover and precipitation, which would cause the weakening of net longwave radiation and incident solar radiation. Consequently the net gain(loss) of heat flux would decrease(increase) to bring sea surface temperature down and create a favorable condition for La Nina. During La Nina, the below-normal surface water temperature would bring about the reducing of sensible and latent heat exchanges and the declining of water vapor content and instability in the atmosphere, and in turn, the weakening of cloud cover and precipitation, which would cause the rising of net longwave radiation and incident solar radiation. Consequently the net gain(loss) of heat flux increases(decreases) to bring sea surface temperature up and create a favorable condition for El Nino. Fig.8 shows the ideal model for this cycle mechanism.

Supposing the averaged maximum of monthly mean temperature anomaly is 1.5°C during El Nino and -1.5°C during La Nina. This anomaly has an influence, with a linear reducing rate downward to 250m in depth, on the ocean surface (0° – 10°S , 180° – 90°W), and the averaged maximum difference of heat budget between El Nino and La Nina is 50Wm^{-2} with a linear reducing rate of heat exchange variation from sea surface temperature abnormal to normal or from sea surface temperature normal to abnormal, we could estimate the period of El Nino-La Nina cycle under the basis of linear progress of air-sea heat exchange as follows:

$$P = 2 \times \frac{0.5 \times (1.5 + 1.5) \times 250 \times 10^2}{0.5 \times 50 \times 1.4331 \times 10^{-3}} = 2.09336 \times 10^6 (\text{min.}) \approx 4(\text{year}).$$

It is promising that the computed result is evidently to be coincided with the observed El Nino-La Nina cycle and furthermore proves the role of air-sea heat exchange in El Nino-La Nina cycle.

V. CONCLUSIONS

Now we could summarize the following conclusions:

(1) Between El Nino and La Nina the differences of heat budget on ocean surface mainly occurred on the equatorial ocean surface, especially on the water area west of the coasts of Ecuador and Peru.

(2) The major distinctions between El Nino and La Nina were the difference of latent heat fluxes and the difference of incident solar radiation fluxes. The difference of sensible heat fluxes and the difference of net longwave radiation fluxes were the next.

(3) The coupling of the complicated air-sea heat exchange is an important physical mechanism for El Nino-La Nina cycle. During El Nino, on the equatorial ocean surface the sensible and latent heat exchanges increased, the net longwave radiation and incident solar radiation decreased. Consequently the net gain(loss) of heat decreased(increased) to lead the declining of sea surface temperature and create a favorable condition for La Nina. During La Nina, the circumstances were opposite.

(4) From heat exchange on ocean surface, the estimated period of El Nino-La Nina cycle is about 4 years.

REFERENCES

- Anderson, D. L. T. and McCreay, J. P. (1985), Slowly propagating disturbances in a coupled ocean-atmosphere model, *J. Atmos. Sci.*, **42**: 615—629.
- Bjernes, J. (1966), A possible response of the atmospheric Hadley circulation to equatorial anomalies of ocean temperature, *Tellus*, **18**: 820—829.
- Budyko, M. I. (1974), *Climate and Life*, Academic Press.
- Bunker, A. (1976), Computation of surface energy flux and annual air-sea interaction cycles of the North Atlantic Ocean, *Mon. Wea. Rev.*, **104**: 1121—1140.
- McCreay, J. P. (1983), A model of tropical ocean-atmosphere interaction, *Mon. Wea. Rev.*, **111**: 370—387.
- McCreay, J. P. et al. (1984), A simple model of El Nino and the Southern Oscillation, *Mon. Wea. Rev.*, **112**: 934—946.
- Monitoring Group of ENSO (1989), Classification and index of El Nino event, *Meteorological Monthly*, **15**:(3) 37—38(in Chinese).
- Ramage, C. S. and Hori, A. M. (1981), Meteorological aspects of El Nino, *Mon. Wea. Rev.*, **109**: 1827—1835.
- Rowntree, P. R. (1972), The influence of tropical east Pacific Ocean temperature on the atmosphere, *Quart. J. Roy. Meteor. Soc.*, **98**: 290—321.
- Schopf, P. S. and Suarez, M. J. (1988), Vacillations in a coupled ocean-atmosphere model, *J. Atmos. Sci.*, **45**: 549—566.
- Wang Shaowu et al. (1986), The western and central Pacific rainfall and the El Nino events, *Acta Meteorologica Sinica*, **44**: 403—410(in Chinese).
- Zhu Yafen and Yang Dasheng(1990), Analysis of air-sea heat exchange during 1983 El Nino, *Acta Oceanologica Sinica*, **12**: 167—178(in Chinese).